



## Progress in Scale Modeling, an International Journal

---

Volume 1

Article 9

---

2020

### Cracking during flame spread over pyrolyzing solids

Yen Nguyen

*Michigan State University*

Indrek S. Wichman

*Michigan State University, wichman@egr.msu.edu*

Thomas J. Pence

*Michigan State University*

Follow this and additional works at: <https://uknowledge.uky.edu/psmij>



Part of the [Architecture Commons](#), [Engineering Commons](#), and the [Physical Sciences and Mathematics Commons](#)

**Right click to open a feedback form in a new tab to let us know how this document benefits you.**

---

#### Recommended Citation

Nguyen, Yen; Wichman, Indrek S.; and Pence, Thomas J. (2020) "Cracking during flame spread over pyrolyzing solids," *Progress in Scale Modeling, an International Journal*: Vol. 1 , Article 9.

DOI: <https://doi.org/10.13023/psmij.2020.09>

Available at: <https://uknowledge.uky.edu/psmij/vol1/iss1/9>

This Research Article is brought to you for free and open access by *Progress in Scale Modeling, an International Journal*. Questions about the journal can be sent to [journal@scale-modeling.org](mailto:journal@scale-modeling.org)

---

## Cracking during flame spread over pyrolyzing solids

### Category

Research Article

### Abstract

A theoretical and numerical model for the degradation of solid materials in combustion is developed. As solid materials are heated by the flame, they undergo an internal thermo-chemical breakdown process known as pyrolysis. As the pyrolysis front propagates into the sample, a charring layer is left behind which contains voids, fractures and defects. Cracks propagate to release tensile stresses accumulated when the sample is losing mass. The crack front may precede the pyrolysis front into the sample. Crack patterns and fracture behaviors vary depending on material properties and heating level and distribution. Cracks cause loss of material integrity by forming isolated loops or fragments. Cracks concentrate the stresses and reduce material ability to withstand external loads. Cracks expose uncharred materials to flame, accelerating combustion. The process is highly nonlinear: crack patterns display fractal behavior. Dimensionless groups that define the model are examined: each yields different crack patterns.

### Keywords

Flame spread, Pyrolyzing materials, Crack formation, Dimensionless groups, Numerical analysis



# Cracking during flame spread over pyrolyzing solids

Yen Nguyen<sup>a</sup>, Indrek S. Wichman<sup>b,\*</sup>, Thomas J. Pence<sup>a</sup>

<sup>a</sup> *Department of Mechanical Engineering, Michigan State University*

<sup>b</sup> *MSU Energy and Automotive Research Laboratories*

E-mail: [wichman@egr.msu.edu](mailto:wichman@egr.msu.edu)

Received June 28, 2020, Accepted July 5, 2020

## Abstract

A theoretical and numerical model for the degradation of solid materials in combustion is developed. As solid materials are heated by the flame, they undergo an internal thermo-chemical breakdown process known as pyrolysis. As the pyrolysis front propagates into the sample, a charring layer is left behind which contains voids, fractures and defects. Cracks propagate to release tensile stresses accumulated when the sample is losing mass. The crack front may precede the pyrolysis front into the sample. Crack patterns and fracture behaviors vary depending on material properties and heating level and distribution. Cracks cause loss of material integrity by forming isolated loops or fragments. Cracks concentrate the stresses and reduce material ability to withstand external loads. Cracks expose uncharred materials to flame, accelerating combustion. The process is highly nonlinear: crack patterns display fractal behavior. Dimensionless groups that define the model are examined: each yields different crack patterns.

*Keywords:* Flame spread; Pyrolyzing materials; Crack formation; Dimensionless groups; Numerical analysis

## Nomenclature

$L$	domain width	$A$	pre-exponent factor
$H$	domain height	$\sigma$	stress tensor
$\alpha$	thermal diffusivity	$u$	displacement in $x$ direction
$T$	solid temperature	$v$	displacement in $y$ direction
$\rho$	solid density		
$\varepsilon$	strain tensor		
$E$	Young's modulus		
$k$	thermal conductivity		
$\gamma$	mass loss coefficient		
$\nu$	Poisson's ratio		
$l$	length of heated region		
$q$	heat flux parameter		

### Subscript

a	activation value
0	initial
c	critical
$x, y$	direction

## Introduction

When solid materials like cellulose, rubber, and plastics are burned they release combustible gases via pyrolysis or evaporation of a liquid pool. The materials lose their structural integrity by charring, deforming and developing defects such as cracks, bubbles and voids. These defects enhance the combustion process by allowing oxygen to travel further into the material. They also allow pyrolysis gases to escape to the surface for subsequent combustion. For pyrolyzing materials, hot gases can force cracks to open by applying elevated

hydrostatic pressures to lateral crack surfaces. The physical mechanism of crack and void formation is understood as follows: The burning sample develops cracks to relieve the tensile stress accumulated by nonuniform mass loss; when internal stresses appear in a sample not subject to external loading there exists a driving field such as temperature, moisture, or pore pressure. Sample constraints or inhomogeneity of the driving field inevitably generate tensile stresses. These crack the sample when specified limiting values are exceeded.

## Mathematical model

Our model includes heat transfer in the solid, material breakdown (pyrolysis) under high temperature, elastic deformation, and crack formation in the solid material. Here, the gas phase provides the external heat flux for the solid phase, which is the focus of our study. We consider the problem over a rectangular  $L \times H$  ( $L$  is length in the  $x$ -direction,  $H$  is depth in the  $y$ -direction) domain. The temperature field  $T(x, y, t)$  is described by the heat conduction equation

$$\frac{\partial T}{\partial t} = \alpha_x \frac{\partial^2 T}{\partial x^2} + \alpha_y \frac{\partial^2 T}{\partial y^2}, \quad (1)$$

where  $\alpha_x$  and  $\alpha_y$  are the thermal diffusivities in the  $x$  and  $y$  directions, respectively. Under a high and constant external heat flux, the solid pyrolyzes according to the following single step reaction equation

$$\frac{\partial \rho}{\partial t} = -A(\rho - \rho_c)e^{-T_a/T}, \quad (2)$$

where  $A$  is the pre-exponential factor,  $T_a$  is the activation temperature and  $\rho_c$  is the lower bound of solid density, or the char density. Because of the two-dimensional nature of the problem, the strain tensor contains only the components  $\varepsilon_{xx}$ ,  $\varepsilon_{xy}$ ,  $\varepsilon_{yx}$ ,  $\varepsilon_{yy}$  and  $\varepsilon_{zz}$ . The stress tensor, for the state of plane stress, only consists of  $\sigma_{xx}$ ,  $\sigma_{xy}$ ,  $\sigma_{yx}$  and  $\sigma_{yy}$ , i.e., we use the plane stress condition,  $\sigma_{zz} = 0$ . When the overall strain is taken to be equal to the sum of a mechanical strain and a shrinkage strain due to loss of mass, the stress-strain relations become

$$\sigma_{ij} = \frac{E}{1+\nu} \varepsilon_{ij} + \left[ \frac{E\nu}{1-\nu^2} (\varepsilon_{kk}) - \frac{E}{1-\nu} \gamma \frac{\rho - \rho_0}{\rho_0} \right] \delta_{ij} \quad (3)$$

$i = 1, 2; j = 1, 2$

where  $i$  or  $j = 1, 2$  represents  $x, y$ . Here  $E$  is the Young's modulus,  $\nu$  is the Poisson's ratio and the coefficient  $\gamma$  couples material mass loss and volume reduction. The displacement fields in the  $x$  and  $y$  directions are denoted by  $u(x, y, t)$  and  $v(x, y, t)$ , respectively. The strains in the  $(x, y)$ -plane are related to  $u$  and  $v$  by the standard relations  $\varepsilon_{xx} = \partial u / \partial x$ ,  $\varepsilon_{yy} = \partial v / \partial y$  and  $\varepsilon_{xy} = (1/2)(\partial u / \partial y + \partial v / \partial x)$ . The stress equations of equilibrium are  $\partial \sigma_{xx} / \partial x + \partial \sigma_{xy} / \partial y = 0$  and  $\partial \sigma_{xy} / \partial x + \partial \sigma_{yy} / \partial y = 0$ , where we have used  $\sigma_{xy} = \sigma_{yx}$ . The stress tensor has three eigenvalues which represent the three principal stresses,  $\sigma_I$ ,  $\sigma_{II}$  and  $\sigma_{III}$ . It is assumed that cracks nucleate and grow whenever the maximum principal stress  $\sigma_p$ , defined as  $\max(\sigma_I, \sigma_{II}, \sigma_{III})$ , attains a threshold value  $\sigma_c$  which is understood in this article as a material constant. Cracks form at locations where  $\sigma_p \geq \sigma_c$ .

We now write the initial and boundary conditions for

the thermal-pyrolysis-stress problem. Initially, the sample has the uniform temperature  $T = T_0$  which is maintained at the two sample lateral sides throughout heating. The lower surface  $y = H$  is insulated so  $\partial T / \partial y = 0$ , while the upper surface is subjected at its surface to a constant heat flux  $q_0$  over the central region of length  $l$ . Thus  $k_y \partial T / \partial y = q_0$  for  $|x - L/2| \leq l/2$ , where  $k_y$  is the  $y$ -direction thermal conductivity. The solid density has uniform initial value  $\rho = \rho_0$ , which gradually decreases to its charring, or minimum value  $\rho_c$ . Regarding the imposed physical boundary conditions, the stress constraint on the lower surface is referred to as a "roller" condition (no deflection in the  $y$ -direction, freedom of movement in the  $x$ -direction, while all three remaining sample sides are unconstrained, or traction free).

## Dimensionless groups

The problem is characterized by three time scales. These scales correspond to heat conduction, heat flux, and chemical reaction. The heat conduction time scale that characterizes Eq. (1) is  $t_{hc} = H^2 / \alpha_y$ . The heat flux time scale that characterizes the relation of thermal boundary conditions to the heat conduction equation Eq. (1) is defined as  $t_{flux} = HT_0 k_y / (\alpha_y q_0)$ . The chemical reaction time scale characterizes the pyrolysis reaction as described by Eq. (2) and is taken as  $t_{chem} = [A \exp(-T_a/T_0)]^{-1}$ .

Our heat conduction- pyrolysis- elasticity problem contains sixteen constants, in which the Poisson's ratio  $\nu$  and the mass loss coefficient  $\gamma$  are already dimensionless. The other fourteen have units composed of four basic units. Of these fourteen,  $q_0$  and  $k_y$  only appears as a ratio, leaving thirteen constants. These constants are  $L$ ,  $H$ ,  $\alpha_x$ ,  $\alpha_y$ ,  $T_0$ ,  $q_0/k_y$ ,  $l$ ,  $\rho_c$ ,  $A$ ,  $T_a$ ,  $\rho_0$ ,  $E$ ,  $\sigma_c$ .

The four basic units can be taken as either length/time/temperature/energy or length/time/temperature/mass. By using the Buckingham  $\pi$  theorem, the thirteen dimensional constants are combined to form nine dimensionless  $\pi$  groups. We choose the following nine  $\pi$  groups to characterize our problem:  $\Pi_1 = H/L$ ,  $\Pi_2 = l/L$ ,  $\Pi_3 = \alpha_y/\alpha_x$ ,  $\Pi_4 = q_0 H / (k_y T_0)$ ,  $\Pi_5 = T_a/T_0$ ,  $\Pi_6 = H^2 A e^{-T_a/T_0} / \alpha_y$ ,  $\Pi_7 = \rho_c/\rho_0$ ,  $\Pi_8 = E/[\rho_0(AH)^2]$ ,  $\Pi_9 = \sigma_c/E$ . The first two groups,  $\Pi_1$  and  $\Pi_2$ , represent the problem geometry. The next two groups,  $\Pi_3$  and  $\Pi_4$ , are properties of the thermal subproblem in which  $\Pi_4$  equals  $t_{hc}/t_{flux}$ . The sixth group is equal to  $t_{hc}/t_{chem}$ . This group, along with  $\Pi_5$ , describes the relationship between the thermal and pyrolysis subproblems. The seventh group defines the extent of pyrolysis while the ninth group specifies the element removal or crack growth criterion. Group  $\Pi_8$  relates material pyrolysis to the stress subproblem. Group  $\Pi_9$ , the ratio of the cracking stress to the elastic modulus, can also be interpreted as the crack resistance

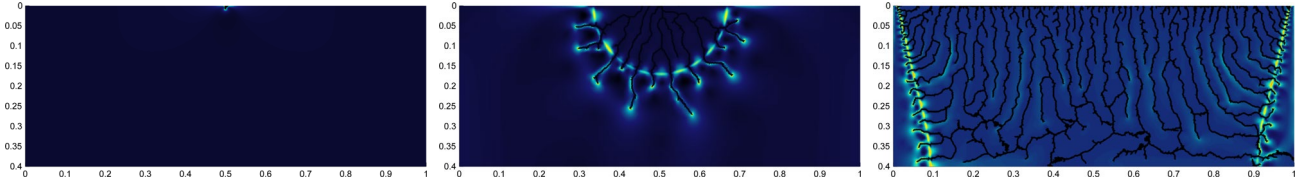


Fig. 1. Vary  $\Pi_2 = l/L$ . Left,  $\Pi_2 = 0.01$ ,  $\Pi_6 = 100\Pi_6^0$ ; Middle,  $\Pi_2 = 0.1$ ,  $\Pi_6 = \Pi_6^0$ ; Right,  $\Pi_2 = 1.0$ ,  $\Pi_6 = \Pi_6^0$ .

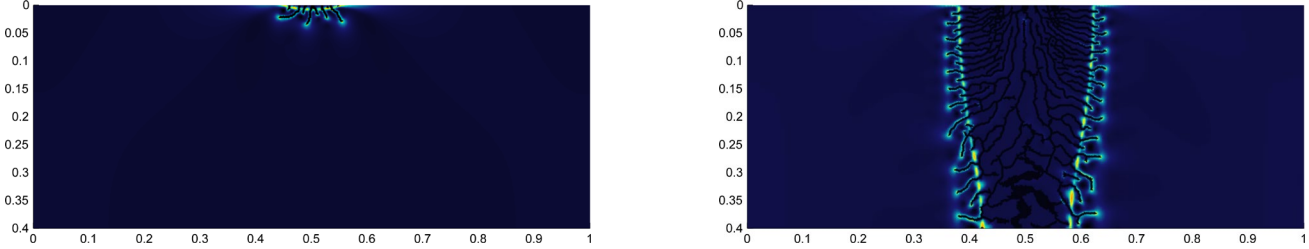


Fig. 2. Vary  $\Pi_3 = \alpha_y/\alpha_x$ . Left,  $\Pi_3 = 0.1\Pi_3^0$ ; Right,  $\Pi_3 = 10\Pi_3^0$ .

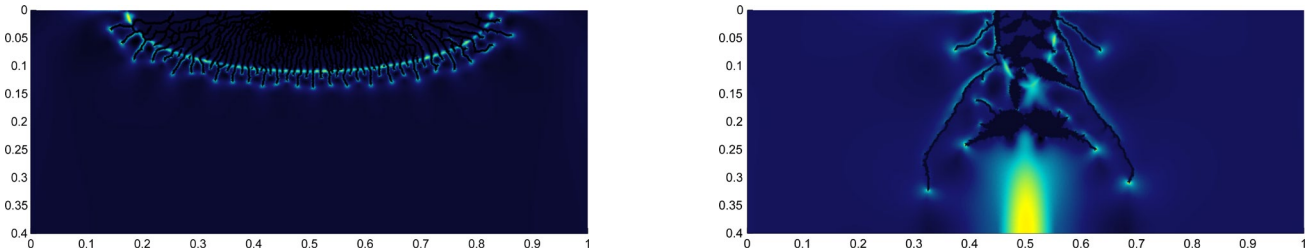


Fig. 3. Vary  $\Pi_3 = \alpha_y/\alpha_x$ . Left,  $\Pi_3 = 0.1\Pi_3^0$  and  $\Pi_6 = 10\Pi_6^0$ ; Right,  $\Pi_3 = 10\Pi_3^0$  and  $\Pi_6 = 0.1\Pi_6^0$ .

parameter. When  $\Pi_9$  is sufficiently large, no cracks can form.

The field of fracture mechanics often separates two distinct process, crack initiation and crack propagation. The theory of thermoelasticity suggests that materials having a high crack initiation resistance also have a high tensile strength, a high thermal diffusivity, a low Young’s modulus and undergo low thermal expansion [1] during heating. During cooling, most materials contract, or shrink, just as the pyrolyzing solid in this study contracts when it loses mass. Thus, the thermal contraction coefficient in cooling is analogous to the current mass loss coefficient because both function as coefficients of the shrinkage stress.

Our problem, characterized by nine  $\pi$  groups, will employ characteristic units from the parameters  $H$ ,  $t_{hc}$ ,  $T_0$  and  $\rho_0$  (length, time, mass and temperature). We let  $\bar{x} = x/H$ ,  $\bar{y} = y/H$ ,  $\tau = t/t_{hc}$ ,  $\theta = (T - T_0)/T_0$ . Then Eq. (1) can be written as:  $\partial\theta/\partial\tau = (\Pi_3\partial^2\theta/\partial\bar{x}^2 + \partial^2\theta/\partial\bar{y}^2)$ . The initial condition for the dimensionless temperature  $\theta$  is  $\theta = 0$ , which is also the boundary condition at the two sides,  $y = 0, L$ . The boundary condition for  $\theta$  on the insulated side is:  $\partial\theta/\partial\bar{y} = 0$ , and on the heated side is:

$$\frac{\partial\theta}{\partial\bar{y}} = \begin{cases} 0 & \text{if } \left| \bar{x} - \frac{1}{2\Pi_1} \right| > \frac{\Pi_2}{2\Pi_1} \\ \Pi_4 & \text{if } \left| \bar{x} - \frac{1}{2\Pi_1} \right| \leq \frac{\Pi_2}{2\Pi_1}. \end{cases}$$

The pyrolysis equation (2) becomes

$$\frac{\partial\bar{\rho}}{\partial\tau} = -(\bar{\rho} - \Pi_7) \frac{1}{\Pi_6} e^{\Pi_5 \left( \frac{\theta}{1+\theta} \right)}.$$

Finally, the stresses are non-dimensionalized with respect to Young’s modulus  $E$  using  $E = (\Pi_8/\Pi_6^2) \exp(2\Pi_5) \rho_0 H^2 / t_{hc}^2$ , viz.  $\bar{\sigma}_{xx} = \sigma_{xx}/E$ ,  $\bar{\sigma}_{yy} = \sigma_{yy}/E$ ,  $\bar{\sigma}_{xy} = \sigma_{xy}/E$ ,  $\bar{\sigma}_{zz} = \sigma_{zz}/E$ ,  $\bar{\sigma}_p = \sigma_p/E$ , where  $\sigma_p$  is the relevant principal stress.

### Numerical results

We use thermo-mechanical properties of a rubber-like material. Also, we use  $q_0/k_y = 1.2 \times 10^5$  K/m as standard values. Subsequently we vary the parameter groups with these as reference values. The sample size is taken to be 5 cm  $\times$  2 cm so  $\Pi_1 = 0.4$ . For rubber-like materials we use  $\nu = 4.5 \times 10^{-1}$  and  $\gamma = 1$ . The reference values of the groups become:  $\Pi_3^0 = 1.0$ ,  $\Pi_4^0 = 4 \times 10^1$ ,  $\Pi_5^0 = 3.15 \times 10^1$ ,  $\Pi_6^0 = 1.0 \times 10^{-3}$ ,  $\Pi_7^0 = 3 \times 10^{-1}$ ,  $\Pi_8^0 = 1.8 \times 10^{-18}$ ,  $\Pi_9^0 = 3.33 \times 10^{-2}$ .

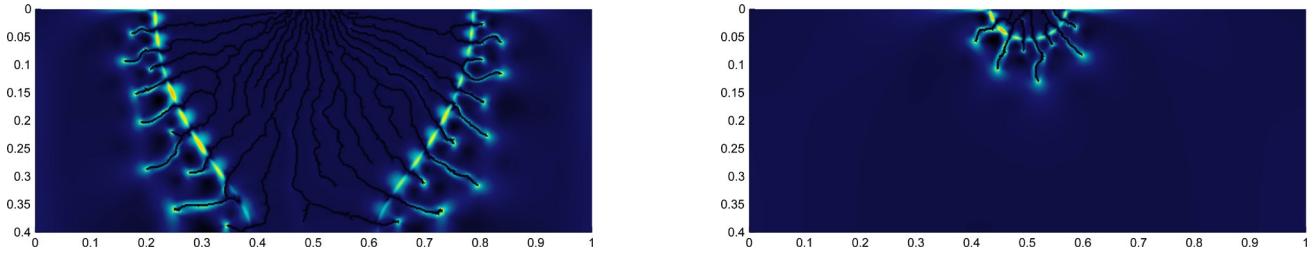


Fig. 4. Vary  $\Pi_4 = q_0H/(k_yT_0)$ . Left,  $\Pi_4 = 2\Pi_4^0$ ; Right,  $\Pi_4 = 0.5\Pi_4^0$ .

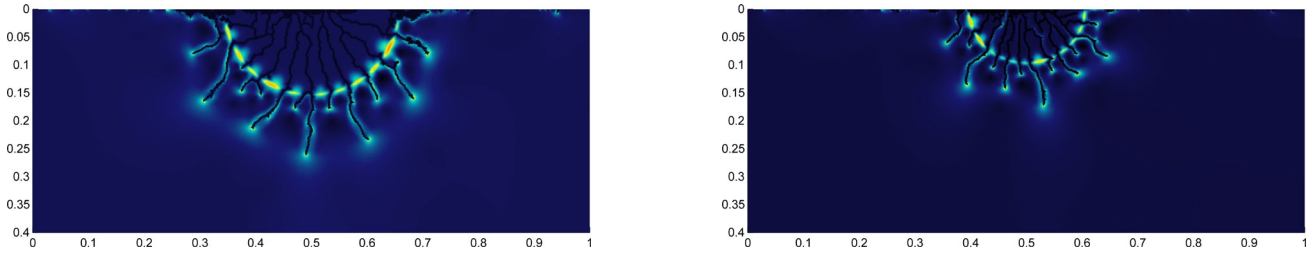


Fig. 5. Vary  $T_a$ .  $\Pi_5 = T_a/T_0$ ,  $\Pi_6 = H^2Ae^{-T_a/T_0}/\alpha_y$ . Left,  $\Pi_5 = 0.9\Pi_5^0$ ,  $\Pi_6 = \Pi_6^0$ ; Right,  $\Pi_5 = 1.1\Pi_5^0$ ,  $\Pi_6 = \Pi_6^0$ .

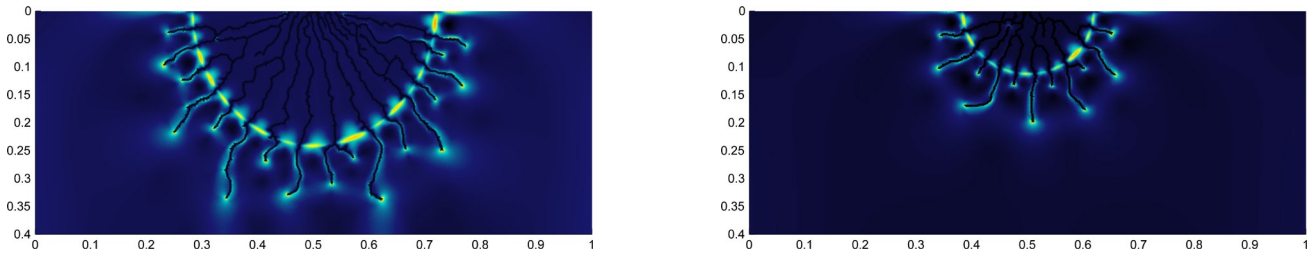


Fig. 6. Vary  $\Pi_6 = H^2Ae^{-T_a/T_0}/\alpha_y$  by varying  $A$ . Left,  $\Pi_6 = 10\Pi_6^0$ ; Right,  $\Pi_6 = 0.1\Pi_6^0$ .

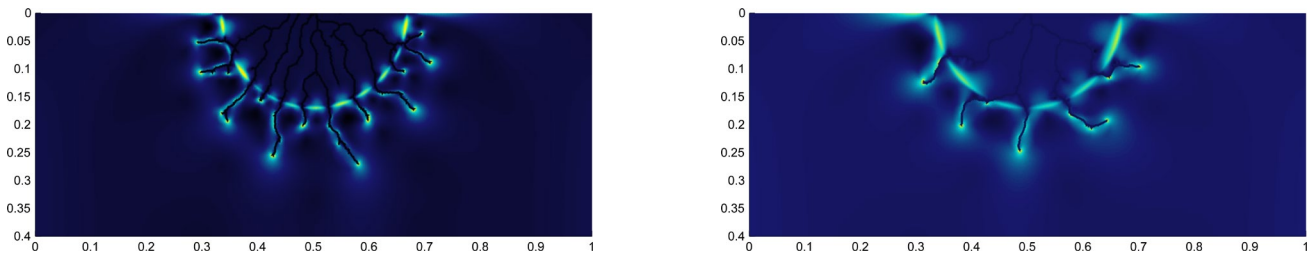


Fig. 7. Vary  $\Pi_9 = \sigma_c/E$ . Left,  $\Pi_9 = \Pi_9^0$ ; Right,  $\Pi_9 = 1.4\Pi_9^0$ . As  $\Pi_9$  increases, fewer cracks form. For very large  $\sigma_c/E$  no cracks will form.

All of the images below show the maximum principal stress field evaluated at the simulation time  $t = 3000$  sec = 50 min. In all cases, the maximum stress is  $\sigma_l$ .

*Vary  $\Pi_2$ .* Group  $\Pi_2$  describes the length  $l$  of the surface over which heat flux is applied. When the heat flux is centered, the cracks propagate radially (Fig. 1 middle,  $\Pi_2 = 0.1$ ). On the other hand, a uniform heat flux over the surface causes crack growth to be vertical (Fig. 1 right,  $\Pi_2 = 1.0$ ). When  $\Pi_2 = 0.1$ , the heat flux may represent a flame whose tip width is  $\approx 5$  mm. In Fig. 1 left,  $\Pi_2 = 0.01$ , a very small heated width, only a small slit forms at the center region of the surface, even with a very high value of  $\Pi_6 = 100\Pi_6^0$  (if  $\Pi_6$  were as

small as the other two figures, there would be no cracks at all).

*Vary  $\Pi_3 = \alpha_y/\alpha_x$ .* As seen from Fig. 2, increasing  $\Pi_3$  enhances heat transfer toward the in-depth ( $y$ ) direction, leading to dramatically different crack patterns (crack growth in-depth) as well as a decrease in the crack spacing in the  $y$ -direction. On the other hand, when  $\Pi_3$  is decreased, heat transfer in the horizontal ( $x$ ) direction is dominant, and the cracks spread horizontally. In Fig. 2 left (right),  $\Pi_3$  decreases (increases) by a factor of 10, the other  $\pi$  groups remaining unchanged. This corresponds to letting the thermal diffusivity in the horizontal direction  $\alpha_x$

increase (decrease) by a factor of 10.

Another way to change  $\Pi_3$  is to change  $\alpha_y$ , which also changes  $\Pi_6 = t_{nc}/t_{chem}$ . From Fig. 2 and Fig. 3, it can be seen that  $\Pi_3$  determines the shape of the crack pattern: both Fig. 2 (Left) and Fig. 3 (Left) have the same  $\Pi_3$ . By contrast, cracks caused by a decrease in  $\alpha_y$  or  $\alpha_x$  lead to more cracks (Fig. 2 (Right) and Fig. 3 (Left)). Fig. 3 (Right) increases  $\alpha_y$  by a factor of 10, keeping  $\alpha_x$  constant.

Vary  $\Pi_4 = q_0H/(k_yT_0)$ . Group  $\Pi_4$  represents heat flux strength. Higher heat fluxes raise the temperature faster, enhance pyrolysis and produce more cracks, see Fig. 4.

Vary activation energy  $T_a$ . Changing  $T_a$  changes both  $\Pi_5$  and  $\Pi_6$ . In Fig. 5 (Left),  $T_a$  is lower by 10 %, whereas in Fig. 5 (Right) it is increased by 10 % over its standard value. As expected, a lower  $T_a$  produces more damage to the sample because it pyrolyzes at a faster rate.

Vary  $\Pi_6$ . Group  $\Pi_6$  characterizes the pyrolysis rate. As  $\Pi_6$  increases, pyrolysis happens at a faster rate, and so does crack propagation as seen from Fig. 6.

Vary  $\Pi_9$ . Since the group  $\Pi_9$  characterizes material strength, samples with higher  $\Pi_9$  produce fewer cracks with larger crack spacing compared with lower strength samples, see Fig. 7.

## Conclusion

This model for crack formation in a pyrolyzing elastic solid generates nine  $\pi$  dimensionless parameter groups. Some are related to geometry, others to heat transfer, some to material chemical breakdown, some to elastic strength parameters, and several linking or coupling these effects. For this reason, the spectrum of material response to heating can be dramatically altered. The heating length scale  $l$  appears only in the ratio  $\Pi_2 = l/L$ . Since the flame scale varies solely through this parameter, this model can potentially be adapted to problems that span the range between very small flames (micro-flames) and very large flames (macro-flames).

## References

- [1] Kingery, W. D., "Factors affecting thermal shock resistance of ceramic materials," J. Am. Ceram. Soc. 38: 3–15, 1995.
- [2] Lah, B., Klinar, D., Likozar, B., "Pyrolysis of natural, butadiene, styrenebutadiene rubber and tyre components: modelling kinetics and transport phenomena at different heating rates and formulations," Chem. Eng. Sci. 87: 1–13, 2013.